

## RESISTANCE CHARACTERISTICS OF SEMI-DISPLACEMENT MEGA YACHT HULL FORMS

**D L Blount and J A McGrath**, Donald L. Blount and Associates, Inc., USA  
(DOI No: 10.3940/rina.ijsect.2009.b2.95)

### SUMMARY

Mega yachts are growing in scale. The combination of cruise and maximum speeds, along with increase in hull lengths result in operational Froude numbers,  $F_{nL}$ , between 0.3 and 1.0. The concentration of current mega yacht projects have  $F_{nL}$  between 0.3 and 0.6 with few approaching  $F_{nL} = 1.0$ . Hull forms with different transverse sections show a variation in resistance characteristics for similar slenderness ratios in this range of Froude numbers. Resistance values among other geometric considerations are sensitive to slenderness ratio and longitudinal center of gravity, LCG. On occasion, LCG shifts, stern wedges and bulbous bows are techniques being employed to achieve minimum resistance for traditional displacement hull forms. However, these techniques need to be approached with caution as transverse instabilities can result at speeds greater than 22 to 25 knots. Hull form variants incorporating flow-separating spray rails become significant at high speeds.

500 mt was selected as being representative of a typical displacement for mega yachts. Model test data were scaled to make comparisons and analyses of bare hull resistance of many available experimental hull series. Thus, this paper addresses resistance variations related to different hull forms, slenderness ratio and other hull characteristics along with suggested design criteria for forecasting the threshold of dynamic transverse stability.

### NOMENCLATURE

|                  |  |
|------------------|--|
| $A_P$            | Projected Bottom Area Bounded by Outer Chine and Transom ( $m^2$ ) |
| AP               | After Perpendicular  |
| B                | Static Waterline Beam (m)  |
| BOA              | Beam Overall (m)   |
| $B_{PT}$         | Maximum Projected Outer Chine Beam at Transom (m)                  |
| $B_{PX}$         | Maximum Projected Outer Chine Beam (m)                             |
| $C_A$            | Correlation Allowance  |
| $C_B$            | Block Coefficient  |
| $C_F$            | Frictional Resistance Coefficient                                  |
| $C_P$            | Prismatic Coefficient  |
| $C_{PE}$         | Prismatic Coefficient of the Entrance                              |
| $C_X$            | Maximum Section Coefficient  |
| $F_{nL}$         | Length Froude Number = $0.514V/(gL)^{1/2}$                         |
| $F_{nV}$         | Volume Froude Number = $0.514 V/(gV^{1/3})^{1/2}$                  |
| FP               | Forward Perpendicular  |
| fot              | Forward of AP or Transom   |
| g                | Acceleration due to Gravity = $9.81(m/sec^2)$                      |
| h                | Mean heave at LCG (m)  |
| $i_e$            | Half Angle of Entrance at Waterline (Deg.)                         |
| L                | Static Waterline Length (m)  |
| LCB              | Longitudinal Center of Buoyancy (m fot)                            |
| $L_E$            | Length of Entrance from FP (m)                                     |
| LCF              | Longitudinal Center of Floatation (m fot)                          |
| LCG              | Longitudinal Center of Gravity (m fot)                             |
| LOA              | Length Overall (m)   |
| $L_p$            | Projected Chine Length (m)   |
| $L/\nabla^{1/3}$ | Slenderness Ratio  |
| R                | Bare Hull Resistance (KN)  |
| Re               | Reynolds Number  |
| T                | Draft (m)  |
| V                | Speed (knots)  |

|           |                                  |
|-----------|----------------------------------|
| W         | Weight of Vessel Displacement    |
| $\beta_M$ | Deadrise Angle Midships (deg)    |
| $\beta_T$ | Deadrise Angle at Transom (deg)  |
| $\tau$    | Mean Pitch (Trim) Angle (deg)    |
| $\nabla$  | Volume of Displacement ( $m^3$ ) |

### 1. INTRODUCTION

The combination of cruise and maximum speeds along with increase in hull length of current mega yacht designs are extending operational Froude numbers,  $F_{nL}$  to a dimensionless speed range between 0.3 and 1.0. In early times,  $F_{nL} = 0.4$  (hull speed) had been noted as being the upper limit for most displacement vessels. The concentration of current mega yacht projects have a  $F_{nL}$  between 0.3 and 0.6 with a few vessels exceeding  $F_{nL} = 1.0$ .

Referenced design documentation has indicated that some form of a relationship between waterline length and displacement, slenderness ratio for example, has a significant influence on hull resistance to weight ratio, R/W, at semi-displacement speeds. There are other factors such as prismatic coefficient,  $C_P$ , and longitudinal center of gravity, LCG, which influence variations in R/W through this speed range. Hull form type may act as an influencing factor on R/W along with other secondary factors.

Systematic experimental study of hull geometry, loading, and distribution of weight exists in the public domain for round-bilge, double-chine and hard-chine vessels in parts of the range of length Froude numbers from 0.3 to 1.0 and higher; round-bilge data bases typically represent

military applications, double chine data reflect high-speed monohull ferries and some motor yachts, and hard-chine data have been related to planing boats and very high-speed motor yachts.

Figure 1 brings some reality to the subject of this paper. R/W from model tests scaled to a displacement of 500 mt are presented graphically for several round bilge and hard chine hulls. (Note that in this paper all model resistance data are for calm, deep water and have been scaled to 500 mt vessels using ATTC 1947 friction line with zero correlation allowance. This approach was used as the majority of public domain information has been published in this format. As model displacements were scaled to 500 mt, full-scale waterline lengths are allowed to vary with a resulting mean of 54.2 m excluding long, slender hulls. Also, full-scale  $R_e$  values are greater than  $1 \times 10^8$  which is in a range whereby  $C_F$  is equivalent for both ATTC 1947 and ITTC 1957 formulations.)

Some highlights in Figure 1 need to be brought to the reader's attention with regard to  $F_{nL}$ . Most modern yachts report their extended range at cruise speeds of  $F_{nL} = 0.22$  to  $0.36$ . Hull speed ( $V/L^{1/2} = 1.34$ ) is defined as  $F_{nL} = 0.40$  and the threshold of planing speeds begins about  $F_{nL} = 1.0$ . Dynamic instabilities have been observed at speeds greater than  $F_{nL} = 0.75$ .

Beyond displacement speeds, the influence of dynamic bottom pressure tends to dominate hydrostatic pressure. In general, instabilities of high-speed motor yachts can be characterized as being non-oscillatory. Non-oscillatory instabilities are observed at moderate speeds (above 22 to 25 knots) and generally occur on relatively heavily-loaded craft. Unstable behavior has been reported in both the transverse (heel) and longitudinal (bow steering) directions with motions ranging from a rapid loss in running trim, progressive heeling to either port or starboard, or a sudden combined roll-yaw motion. Usually this type of instability can be remedied by reducing the operational speed of the vessel below 22/25 knots.

Figure 2 is a repeat of Figure 1 with the performance of some modern motor yachts located at their reported maximum speed. Recent motor yachts such as 72.8 m Predator and 73.3 m Silver report maximum speeds of  $F_{nL} = 0.54$  and  $0.57$ , respectively. 37.5 m Ermis<sup>2</sup> reports cruise speed of  $F_{nL} = 1.00$  and maximum speed of  $F_{nL} = 1.62$ ; the fastest motor yacht is 41.5 m Fortuna at  $F_{nL} = 1.89$ . The operational speed range of Destriero during its Atlantic crossing record run is noted to be  $F_{nL} = 0.89$  at the start and  $F_{nL} = 1.27$  on arrival in England. Other known mega yacht projects being developed will have extended range at cruise speeds greater than  $F_{nL} = 0.35$  and maximum speeds approaching  $F_{nL} = 1.0$ .

With the technical challenges related to minimizing hull resistance from  $F_{nL} = 0.30$  to  $1.00$ , a study of public domain data was undertaken to explore the subtleties

necessary for defining criteria for low-drag, dynamically-stable hull forms. However, it is important to remember that while a goal of achieving low-hull resistance in order to have a fast yacht with good fuel economy, speed in a seaway without adequate dynamic stability and good ride quality can result in an ill-served client. The hope here is to dissect for semi-displacement speeds the technology bounded by the round bilge and hard chine R/W curves to provide informed guidance for this component of the design process.

Two final points: The analysis of these data is continuing to identify other aspects for possible design guidance. Should sufficient findings emerge, a follow-on paper will be offered. Also, some of the information included in this paper may have application to the design of demi-hulls of catamarans excluding the interactions of the transverse and longitudinal proximity of the two hulls.

## 2. APPROACH

References were collected which reported significant experimental data whereby systematic variation in hull geometry, loading and mass distribution had been studied for  $F_{nL} > 0.30$ . The referenced data that were used for this paper have, in Appendix A, body plans for the parent hulls along with a brief summary of the variables studied in each series. Recent model test data for individual hull designs not included in Appendix A have also been used to independently validate trends and magnitude of resistance data for 500 mt vessels.

The format selected in 1910 to 1914 for reporting the Taylor Standard Series focused on presenting the effect of changes to residual resistance resulting from variables studied. This format has influenced data reporting of other test series as well as benefitting selection of hull dimensions for minimum residual resistance. For comparisons of performance for several vessels utilizing Taylor's format of residual resistance per ton of displacement, wetted surface must be appropriately taken into account.

Thus, for comparative analyses for this paper, we elected to use total bare hull resistance to weight ratio which takes into account both frictional and residual resistance.

## 3. INFLUENCING RESISTANCE FACTORS

In the semi-displacement speed range between  $F_{nL} = 0.3$  and  $1.0$  factors other than traditional displacement hull form coefficients have influence on total bare hull resistance. Slenderness ratio is clearly the dominate factor with LCB/L following in significance. L/B is of lesser significance while tertiary hull form coefficients may also have some affect. It has been, however, difficult to define these tertiary relationships to resistance due to the nature of the organization, execution and original reporting of these test series.

### 3.1 SLENDERNESS RATIO

At  $F_{nL} = 0.3$  the predominately lowest resistance characteristics are attained with round-bilge, displacement hull forms. There are, however, widely-dispersed groups of data at this relatively low dimensionless speed and again at the high speed of  $F_{nL} = 1.0$ . These clusters of data in some regards are related to hulls operating outside of their design speed range. Between these low and high speeds, hull-form variants displayed rather orderly trends with changes in speed. With increase of speed some clear demarcation between round-bilge, double-chine and hard-chine hulls begins to be established. In Figure 3, R/W data of all nine series are plotted for  $F_{nL} = 0.6$  with separate symbols for round-bilge, double-chine and hard-chine hull forms. The trends for each hull form are clearly discernable.

In addition, for speeds below  $F_{nL} = 0.5$  some additional very slender round-bilge hull data were available which confirms that minimum R/W occurs for a slenderness ratio of about 10 or 11. For high values of slenderness ratio (about  $L/\nabla^{1/3} = 18$ ) frictional resistance increases slowly at a greater rate than residual resistance reduces.

The NPL (round bilge) data in Figure 4 show the general trends foreseen in other series. It is noted that R/W for  $F_{nL} = 0.3$  and  $0.4$  are relatively constant for a wide variation in  $L/\nabla^{1/3}$ . R/W then begins to increase significantly with reduction in  $L/\nabla^{1/3}$  below 7.0 for speeds of  $F_{nL} = 0.5$  and greater; for  $F_{nL}$  increases between 0.4 and 0.5 there are especially significant increases of R/W with reduction in  $L/\nabla^{1/3}$ .

Appendix B provides a table of minimum R/W attained for notional 500 mt displacement vessels for round-bilge, double-chine and hard-chine hull forms for  $F_{nL}$  from 0.4 to 1.0 as a function of slenderness ratio. This table provides a benchmark by which naval architects may evaluate the relative resistance of new hull designs. These tabular results indicate attainable resistance for these three hull forms without yet defining other geometric and weight coefficients/characteristics.

### 3.2 LCB/L

Not all of the series varied the longitudinal position of center of gravity or buoyancy (most notably Taylor's series), but within the three hull forms there were sufficient data to establish trends and/or optimum positions for LCB/L. Figure 5 defines the approximate locus of minimum R/W with a dashed line. The R/W penalty at high speeds is readily seen with a forward or aft mislocation of LCB or LCG. At low displacement speeds the minimum R/W is achieved with the center of weight near midships.

It is seen in Figure 6 how R/W varies with LCB/L for variation in  $L/\nabla^{1/3}$  for a constant speed,  $F_{nL} = 0.6$ . At this speed R/W is much less dependent on LCB/L than it is influenced by the magnitude of  $L/\nabla^{1/3}$ . And comparing data between Figures 5 and 6 it can be seen that the minimum value of R/W at  $F_{nL} = 0.6$  corresponds approximately to  $L/\nabla^{1/3} = 9.0$  at LCB/L of 40% fot.

### 3.3 L/B

Length-to-beam ratio is not totally independent of slenderness ratio. Vessels with the same waterline length, but having different waterline beams most likely will not have the same slenderness ratios due to different displacements. The lesser beam hull does not have the capacity/volume to be densely equipped and/or filled with consumables. Thus, at increasing semi-displacement speeds L/B becomes a secondary parameter relative to resistance in calm, deep water as seen in Figure 7.

### 3.4 OTHER PARAMETERS

Traditional displacement hull form coefficients such as  $C_B$ ,  $C_P$ ,  $C_X$ ,  $B/T$ ,  $C_{PF}$ ,  $L_E/L$ ,  $i_c$ , etc. have reduced significance for optimizing total resistance as a vessel approaches the planing speed threshold  $F_{nL} = 1.0$ .

Some guidance can be provided for a limited range of some hull form coefficients, but must be used with caution as these data summaries are subsets of single series experiments. Also, these data were reported in various references in different formats precluding direct comparison.

- Half angle of entrance at the waterline,  $i_c$ , from one series varying 3.7 to 7.8 degrees showed no effect on R/W for speeds from  $F_{nL} = 0.4$  to 0.7 for  $L/\nabla^{1/3}$  from 8.0 to 9.6. A second hull series with  $i_c$  varying from 6.5 to 11.3 degrees shows little effect on R/W for  $i_c$  less than 8 degrees for speeds up to  $F_{nL} = 0.8$ . For  $i_c$  above 8 degrees the change in R/W increases on the order of 0.01 for  $i_c$  up to 11+ degrees for intermediate speeds of  $F_{nL} = 0.5$  and  $F_{nL} = 0.6$ . There is less of a change of R/W (less than 0.006) related to  $i_c$  above and below these speeds.
- Length of entrance of the hull,  $L_E/L$  and the longitudinal prismatic coefficient of the entrance,  $C_{PE}$  are not independent of  $i_c$ . The trends for speeds of  $F_{nL} = 0.3$  and  $0.4$  suggest values of  $C_{PE} = 0.59$  with  $L_E/L = 0.50$  favor low R/W; values of  $C_{PE} = 0.62$  with  $L_E/L = 0.55$  favor lower R/W for speeds  $F_{nL} > 0.4$  up to  $F_{nL} = 0.54$ .
- Block coefficient,  $C_B$  seems to have secondary influence for optimizing high-speed hull forms as high Froude number vessels tend to have relatively shallow draft. However, from information gathered during this study, values of  $C_B$  varied between 0.37

and 0.46 for the hulls with relatively low R/W with an average of 0.43.

- A seakeeping study has been conducted on naval vessels to evaluate the relationship between LCB and LCF with regard to ride quality. It was found that a round-bilge hull having LCF 11% of L aft of LCB has reduced pitch in head seas, pitch resonance occurs at low speeds, and low R/W for speeds from  $F_{nL} = 0.3$  up to  $F_{nL} = 0.54$ .

#### 4. DYNAMIC INSTABILITY

Dynamic instability referred to herein is related to speed-induced bow diving, heel and/or coursekeeping changes coupled with yaw which are non-oscillatory (these instabilities are distinctly different for oscillatory instabilities such as porpoising or chine walking.) These instabilities result when a heavily-loaded vessel operates at speeds in excess of 22 to 25 knots and the velocity of water at the surface of the hull generates low (suction) pressures. Should these dynamic pressures occur asymmetrically, as might happen in a seaway, one side of the vessel may be sucked down (heels) and remain in that attitude until speed is reduced. The heeled attitude will induce a yaw moment resulting in course deviation/bow steering.

Round-bilge vessels tend to be more susceptible to this form of instability than hard- or double-chine hulls, although the latter two may also exhibit this characteristic at high speed when overloaded and/or operated with a low trim by the bow. Whenever a round-bilge yacht is powered so that it may operate at speeds greater than  $F_{nL} = 0.75$  or chine hulls have operational conditions for LCG/L approaching 45%  $F_{nL}$  or greater, then it is recommended model experiments be conducted to evaluate the potential for dynamic instabilities.

On occasion, hulls designed to operate in the speed range above  $F_{nL} = 0.5+$  incorporate stern wedges, hook in afterbody buttocks and/or trim devices to produce bow-down moments with a goal of reduction in resistance. These speed increase techniques can also result in dynamic instability and should be evaluated for potential impact on stability.

#### 5. DESIGN GUIDANCE

The essence of this investigation was to summarize guidelines to reduce the time, given client requirements, to select hull forms and overall dimensions for concept and preliminary designs resulting in near to optimum performance. Data presented thus far has focused on minimum calm, deep water resistance. There are other practical issues summarized in Figure 8; speed ranges whereby round-bilge, double-chine and hard-chine hull forms may be the preferred choice are indicated. When it is beneficial to incorporate other significant features such as bulbous bows, transom sterns, afterbody wedges or hook in the buttocks and/or straight buttocks aft are

suggested. Design values for  $C_p$  are indicated here for all but heavily-laden trawlers which can be found elsewhere in other works.

An especially important feature for high-speed round-bilge hulls is longitudinal flow separators/chines/knuckles beginning at the stem above the static waterline, continuing aft to at least midships below the waterline. The placement of this flow separator in elevation relative to the bilge radius should be carefully considered as it serves competing technical purposes; both flow separation of the bow wave and below-water flow separation so as to minimize the probability of dynamic instability.

Fortunately, many aspects of these design guidance elements do not degrade the seakeeping qualities of these high-performance yachts.

#### 6. CONCLUDING REMARKS

Low resistance is only a component of the overall design process as a holistic solution needs to be found at the end of the design spiral. An optimum solution depends on client requirements which often directly or indirectly include one of the following: Minimum weight to maximize performance, least construction cost, or least annual cost of operation. Moving around the design spiral and considering the interactive nature of technologies encountered, the design team leader makes the necessary and compromising decisions to bring the best yacht to fruition, most likely resulting in a hull design having resistance slightly higher than minimum possible within the boundaries of known hydrodynamic technology.

#### 7. REFERENCES

1. TAYLOR, D.W., 'The Speed and Power of Ships', 3<sup>rd</sup> Edition, U.S. Government Printing Office, 1943.
2. GERTLER, M., 'The Prediction of Effective Horsepower of Ships by Methods in Use at the David Taylor Model Basin', *David Taylor Model Basin Report 576*, December 1947.
3. NORDSTROM, H.F., 'Some Tests With Models of Small Vessels', *SSPA Report No. 19*, 1951.
4. GERTLER, M., 'A Reanalysis of the Original Test Data for the Taylor Standard Series', *David Taylor Model Basin Report 806*, March 1954.
5. CLEMENT, E.P. AND BLOUNT, D.L., 'Resistance Tests of a Systematic Series of Planing Hull Forms', *SNAME Transactions*, 1963.
6. Graff, W., Kracht, A. and Weinblum, G. 'Some Extensions of D.W. Taylor's Standard Series', *SNAME Transactions*, 1964.

7. YEH, H.Y.H., 'Series 64 Resistance Experiments on High-Speed Displacement Forms', *Marine Technology*, July 1965.
8. RIDGELY-NEVITT, 'The Resistance of a High Displacement-Length Ratio Trawler Series', *SNAME Transactions*, 1967.
9. Scholars, R.E., 'An Investigation of the Performance Characteristics of a Long, Slender Hull', *Trident Scholar Report, U.S. Naval Academy*, May 1968.
10. Marwood, W.J. and Bailey, D., 'Transverse Stability of Round-Bottomed High Speed Craft Underway', *NPL Ship Report 98*, October 1968.
11. MARWOOD, W.J. AND BAILEY, D., 'Design Data for High-Speed Displacement Hulls of Round-Bilge Form', *National Physical Laboratory, Report 99*, February 1969.
12. BARNABY, K.C., 'Basic Naval Architecture', *Hutchinson Scientific and Technical, London, 6<sup>th</sup> Edition*, November 1969.
13. HUBBLE, E.N., 'Resistance of Hard-Chine, Stepless Planing Craft with Systematic Variation of Hull Form, Longitudinal Center of Gravity and Loading', *Naval Ship Research and Development Center Report 4307*, April 1974.
14. BAILEY, D., 'Performance Prediction – Fast Craft', *RINA Occasional Publication No. 1*, November 1974.
15. BAILEY, D., 'The NPL High Speed Round Bilge Displacement Hull Series', *Maritime Technology Monograph, No. 4*, 1976.
16. KEUNING, J.A. and GERRITSMA, J., 'Resistance Tests of a Series of Planing Hull Forms with 25 Degrees Dead-Rise Angle', *ISP, Vol. 29, No. 337*, September 1982.
17. BEYS, P.M., 'Series 63 – Round Bottom Boats', *Stevens Institute of Technology, Davidson Laboratory Report 949*, 1963.
18. GRIGOROPOULOS, G.J. and LOUKAKIS, T.A., 'Resistance of Double-Chine, Large, High-Speed Craft', *Bulletin de L'Association Technique Maritime et Aeronautique, ATMA Vol. 99, Paris*, June 1999.
19. RADOJCIC, D., GRIGOROPOULOS, G.D., RODIC, T., KUVELIC, T., and DAMALA, D.P., 'The Resistance and Trim of Semi-Displacement, Double Chine, Transom-Stern Hull Series', *FAST 2001, Vol. III*, 2001.
20. KOWALYSHYN, D.H. AND METCALF, B., 'A USCG Systematic Series of High Speed Planing Hulls', *SNAME Transactions*, 2006.
21. KATAYAMA T., FUJIMOTO, M., and YOSHIHO, I., 'A Study On Transverse Stability Loss of Planing Craft at Super High Forward Speed', *STAB2006*, September 2006.



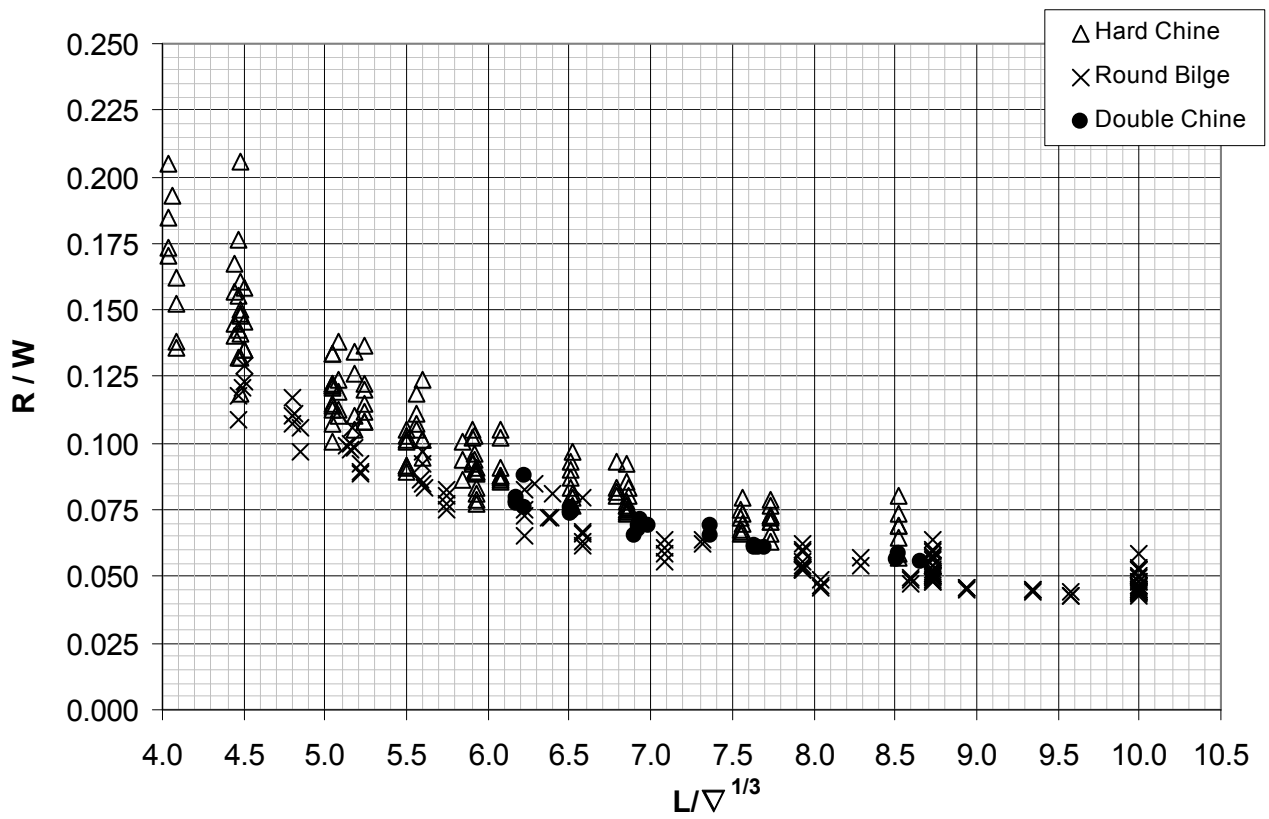


Figure 3: R/W Characteristics for Hard-Chine, Round-Bilge and Double-Chine Hulls at  $F_{nL} = 0.6$

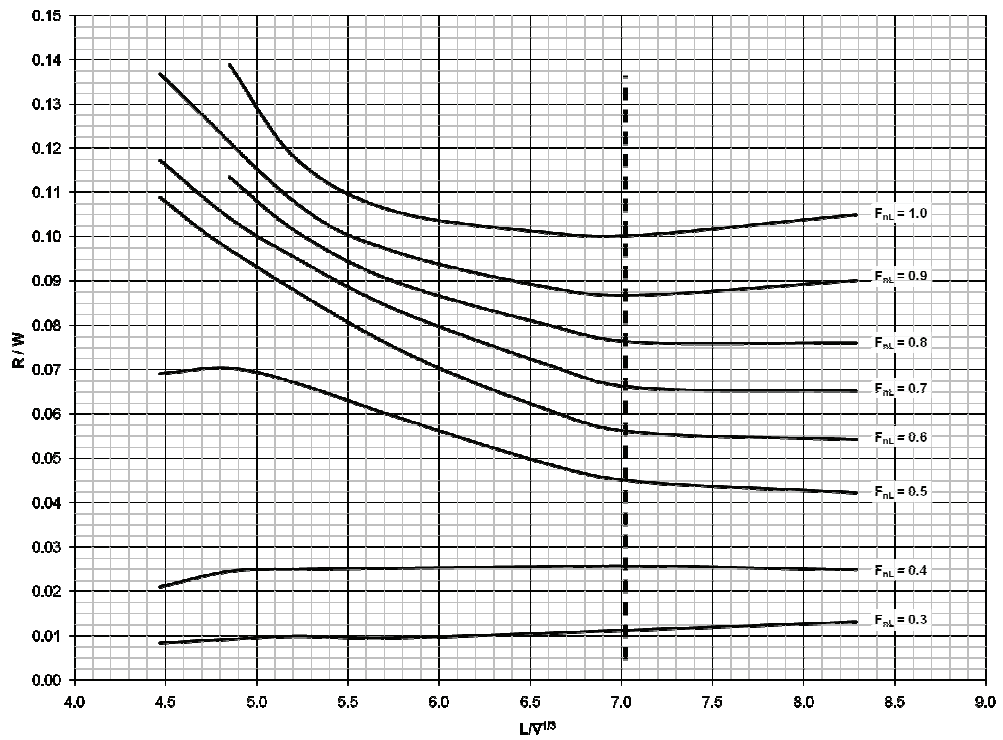


Figure 4: General Trends of R/W Versus  $L/\nabla^{1/3}$  for NPL Round-Bilge Data

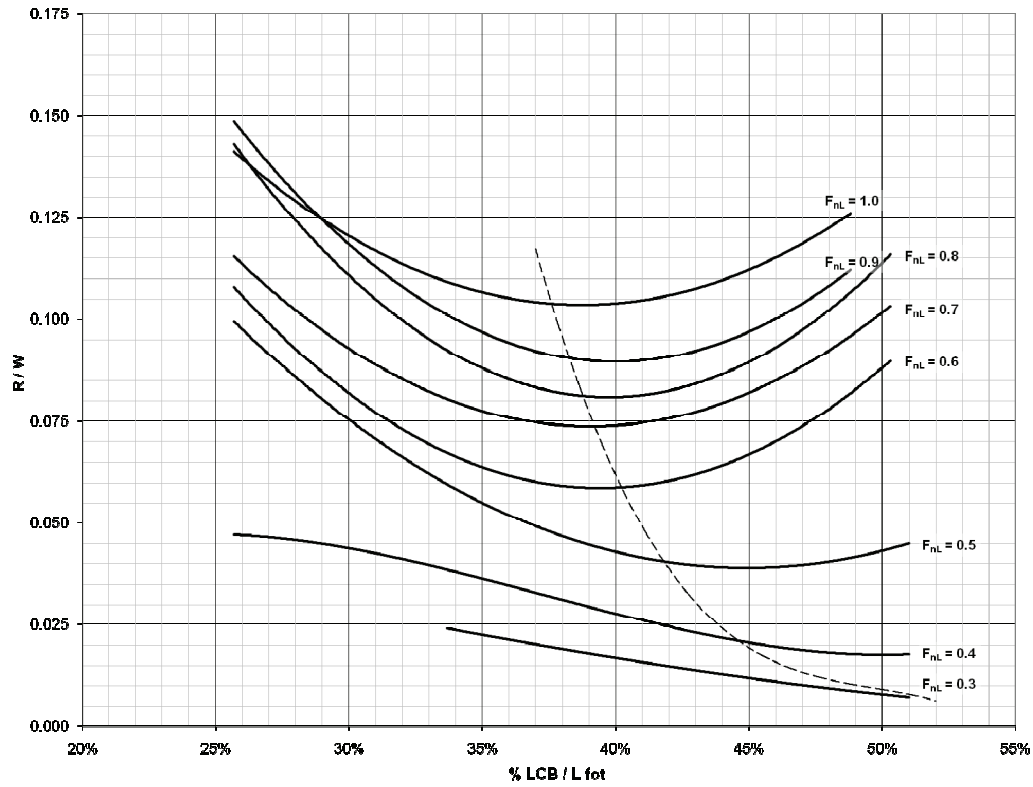


Figure 5: Locus of Minimum R/W Versus LCB/L for a Range of Speeds

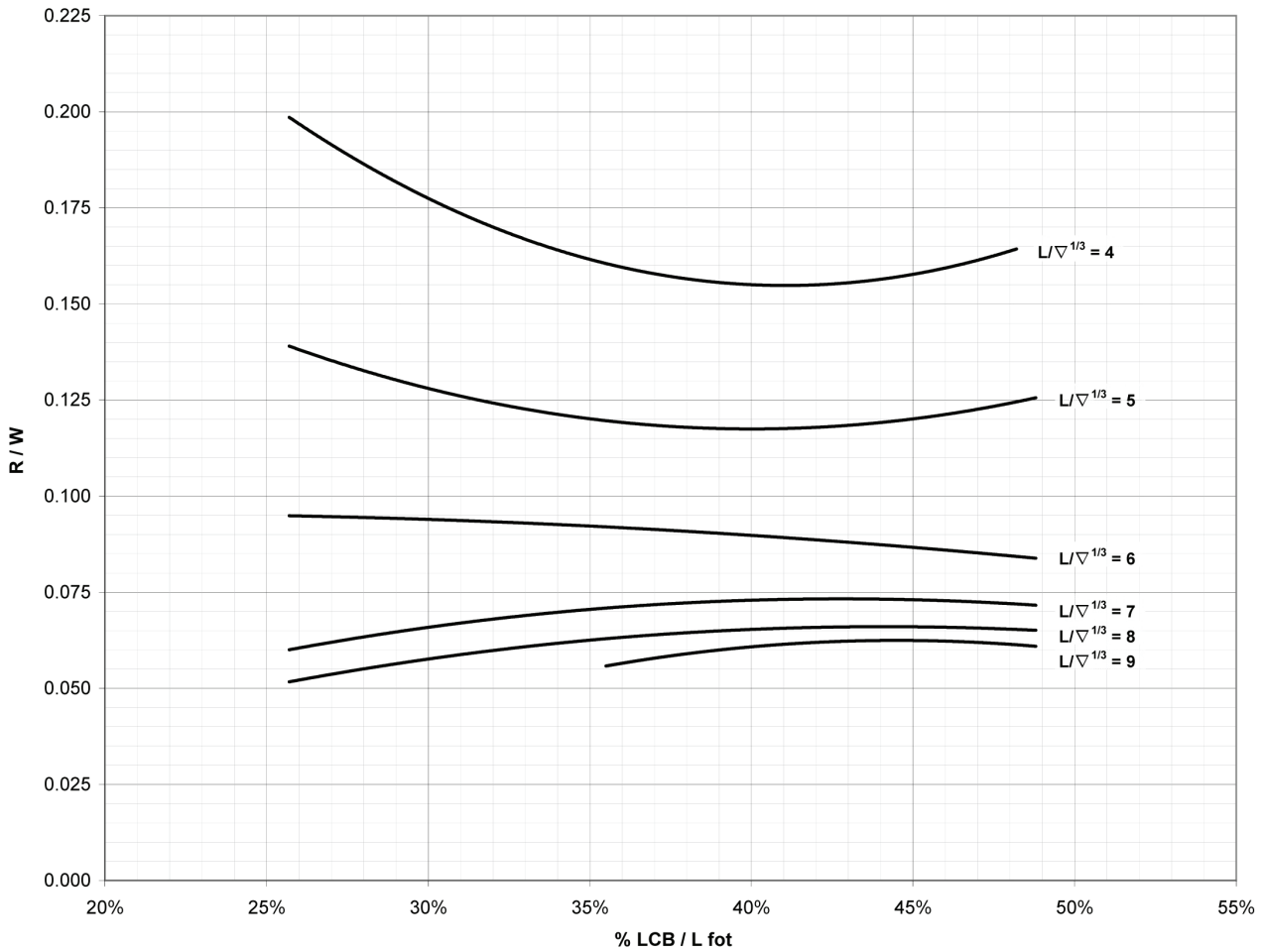


Figure 6: R/W Versus LCB/L for a Range of  $L/\nabla^{1/3}$  for  $F_{nL} = 0.6$



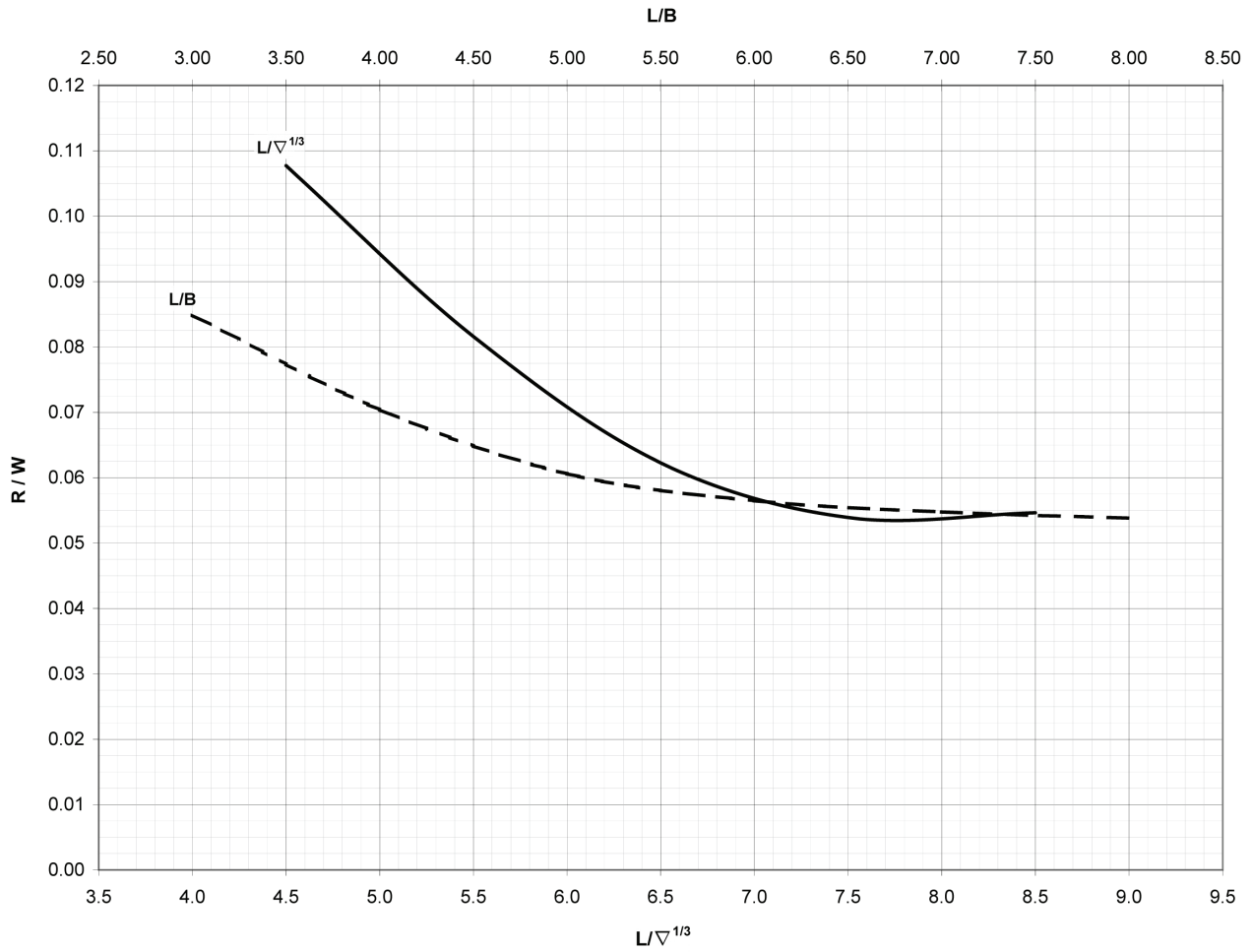


Figure 7: Comparative R/W Relationship with L/B and  $L/\nabla^{1/3}$  at  $F_{nL} = 0.6$  for an NPL Round-Bilge Hull

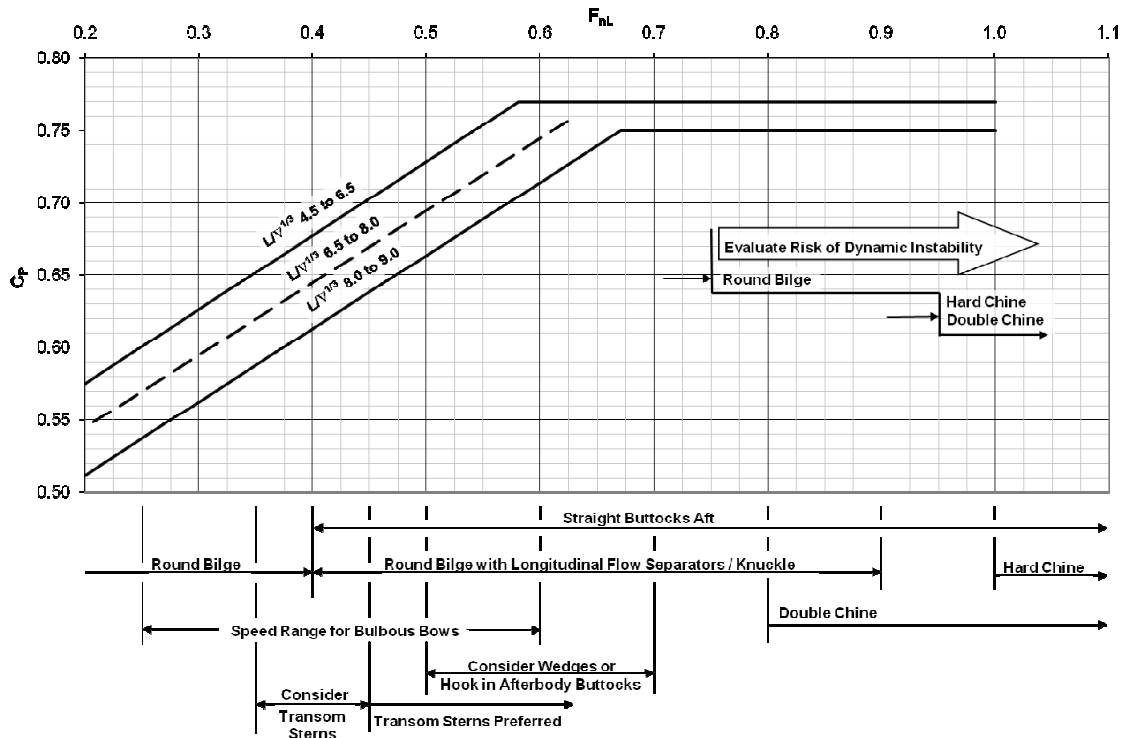
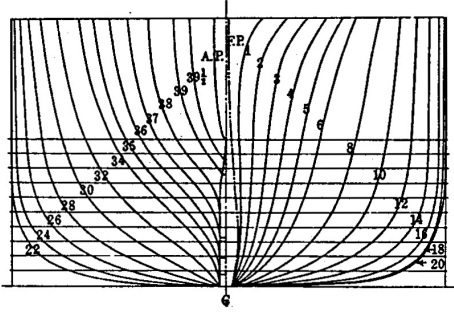
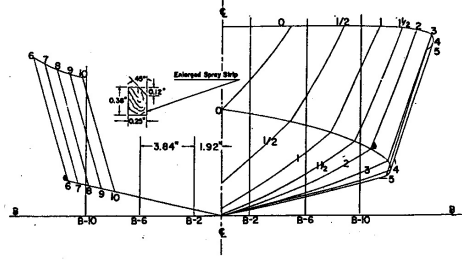
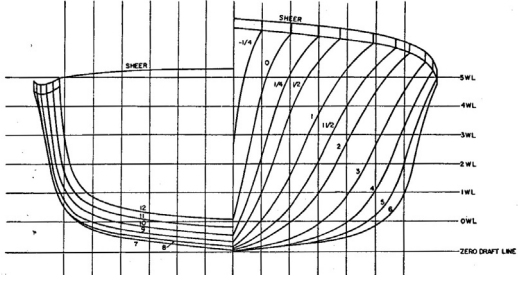
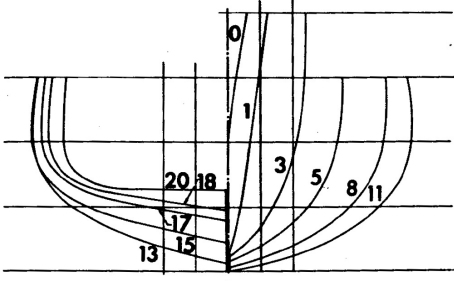
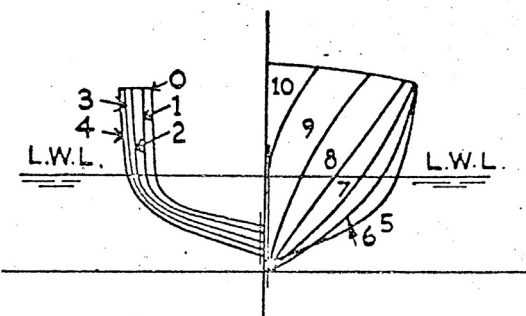
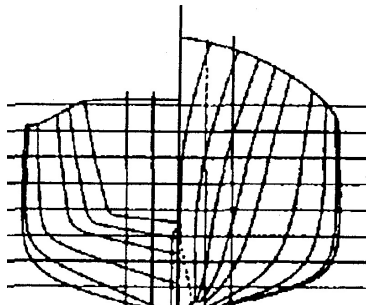
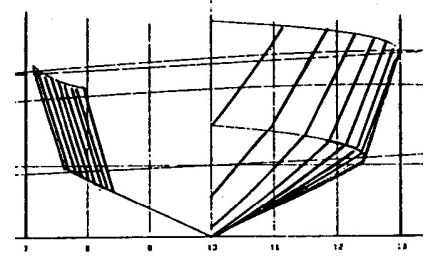
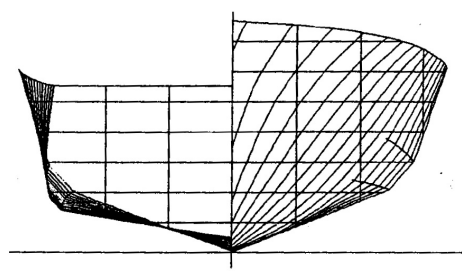
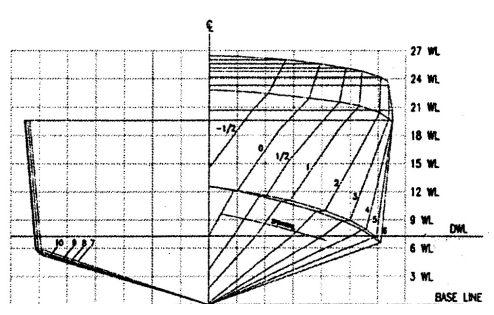


Figure 8 – Design Guidance

APPENDIX A

PARENT BODY PLANS OF SYSTEMATIC SERIES' TESTS

|   |   |
|---|---|
|    | <p><i>TAYLOR STANDARD SERIES</i><br/>                     145 Models<br/>                     Testing 1907 to 1914<br/>                     D.W. Taylor<br/>                     Maximum Speed <math>F_{nL} = 0.60</math><br/> <u>Fixed Parameters</u><br/> <math>LCB/L = 0.50, L_E/L = 0.50, C_X = 0.925</math><br/> <u>Variable Parameters</u><br/> <math>F_{nL}, L/\nabla^{1/3}, B/T, C_B, C_P</math></p>  |
|   | <p><i>DTMB SERIES 62</i><br/>                     5 Models<br/>                     Published 1963<br/>                     E. Clement &amp; D. Blount<br/>                     Maximum Speed <math>F_{nL} = 3.00</math><br/> <u>Fixed Parameters</u><br/> <math>\beta_T = 12.5^\circ</math><br/> <u>Variable Parameters</u><br/> <math>F_{nL}, L/\nabla^{1/3}, L/B, LCG, LCB/L</math></p>  |
|  | <p><i>DTMB SERIES 63</i><br/>                     5 Models<br/>                     Published 1963<br/>                     P. Beys<br/>                     Maximum Speed <math>F_{nL} = 0.88</math><br/> <u>Fixed Parameters</u><br/>                     L, static trim<br/> <u>Variable Parameters</u><br/> <math>F_{nL}, L/\nabla^{1/3}, L/B, LCG, C_B, C_P, C_X</math></p>  |
|  | <p><i>DTMB SERIES 64</i><br/>                     27 Models<br/>                     Published 1965<br/>                     H.Y.H. Yeh<br/>                     Maximum Speed <math>F_{nL} = 1.50</math><br/> <u>Fixed Parameters</u><br/> <math>L, L_E/L = 0.60, LCF/L = 0.40</math> fwd AP, <math>LCB/L = 0.43</math> fwd AP, <math>C_P = 0.63, C_{PF} = 0.52, C_W = 0.76</math><br/> <u>Variable Parameters</u><br/> <math>F_{nL}, L/\nabla^{1/3}, L/B, C_B, B/T, C_X, i_e</math></p> |

|  |  |
|--|--|
|  <p>A technical drawing of a hull cross-section for the NPL series. The hull is shown on a horizontal base line. The waterline is indicated by two horizontal lines labeled 'L.W.L.' on either side. The hull shape is defined by a series of numbered points: 0, 1, 2, 3, 4, 5, 6, 7, 8, 9, and 10. Points 0-4 are on the left side, and points 5-10 are on the right side. The hull has a relatively flat bottom and a rounded, slightly flared stern.</p>  | <p><b>NPL SERIES</b><br/>                 22 Models<br/>                 Published 1969 &amp; 1976<br/>                 D. Bailey, et al<br/>                 Maximum Speed <math>F_{nL} = 1.20</math><br/> <u>Fixed Parameters</u><br/> <math>C_B = 0.40</math>, <math>C_P = 0.69</math>, <math>C_X = 0.57</math>, <math>LCB/L = 0.44</math> fwd AP,<br/> <math>L_E/L = 0.60</math><br/> <u>Variable Parameters</u><br/> <math>F_{nL}</math>, <math>L</math>, <math>L/B</math>, <math>B/T</math>, <math>L/\nabla^{1/3}</math>, <math>i_c</math></p>   |
|  <p>A technical drawing of a hull cross-section for the DTMB Naval LCB-LCF Mini-Series. The hull is shown on a horizontal base line. The hull shape is defined by a grid of lines. The hull has a flat bottom and a rounded, slightly flared stern.</p>   | <p><b>DTMB NAVAL LCB-LCF MINI-SERIES</b><br/>                 9 Models<br/>                 Published 1970<br/>                 M. Lasky<br/>                 Maximum Speed <math>F_{nL} = 0.54</math><br/> <u>Fixed Parameters</u><br/> <math>L/B</math>, <math>B/T</math>, <math>\nabla</math>, <math>C_B = 0.47</math>, <math>C_P = 0.58</math>, <math>C_X = 0.81</math><br/> <u>Variable Parameters</u><br/> <math>F_{nL}</math>, <math>C_{PF}</math>, <math>L_E/L</math>, <math>i_c</math>, <math>LCB/L</math>, <math>LCF/L</math></p>  |
|  <p>A technical drawing of a hull cross-section for the Delft Series. The hull is shown on a horizontal base line. The hull shape is defined by a grid of lines. The hull has a flat bottom and a rounded, slightly flared stern.</p>  | <p><b>DELFT SERIES (RELATED TO DTMB SERIES 62)</b><br/>                 5 Models<br/>                 Published 1982<br/>                 J. Keuning &amp; J. Gerritsma<br/>                 Maximum Speed <math>F_{nL} = 1.65</math><br/> <u>Fixed Parameters</u><br/> <math>\beta_T = 25.0^\circ</math><br/> <u>Variable Parameters</u><br/> <math>F_{nL}</math>, <math>L/\nabla^{1/3}</math>, <math>L/B</math>, <math>LCG</math>, <math>LCB/L</math></p>  |
|  <p>A technical drawing of a hull cross-section for the NTUA Series. The hull is shown on a horizontal base line. The hull shape is defined by a grid of lines. The hull has a flat bottom and a rounded, slightly flared stern.</p>  | <p><b>NTUA SERIES</b><br/>                 5 Models<br/>                 Published 1999 &amp; 2001<br/>                 G. Grigoropoulos, et al<br/>                 Maximum Speed <math>F_{nL} = 1.10</math><br/> <u>Fixed Parameters</u><br/> <math>\beta_T = 10^\circ</math><br/> <u>Variable Parameters</u><br/> <math>F_{nL}</math>, <math>L/\nabla^{1/3}</math>, <math>B/T</math>, <math>L/B</math>, <math>LCB/L</math></p>  |
|  <p>A technical drawing of a hull cross-section for the USCG Series. The hull is shown on a horizontal base line. The hull shape is defined by a grid of lines. The hull has a flat bottom and a rounded, slightly flared stern. The diagram includes a vertical axis labeled 'ε' and a horizontal axis labeled 'DML'. The hull shape is defined by a series of numbered points: 3 WL, 6 WL, 9 WL, 12 WL, 15 WL, 18 WL, 21 WL, 24 WL, and 27 WL. The hull has a flat bottom and a rounded, slightly flared stern.</p> | <p><b>USCG SERIES</b><br/>                 4 Models<br/>                 Published 2006<br/>                 D. Kowalyshyn &amp; B. Metcalf<br/>                 Maximum Speed <math>F_{nL} = 2.54</math><br/> <u>Fixed Parameters</u><br/> <math>C_B = 0.43</math>, <math>LCB/L = 0.38</math>, <math>\beta_T = 16.6^\circ</math>, <math>C_P = 0.70</math>, <math>LCF/L = 0.40</math>, <math>i_c = 19.5^\circ</math>**<br/> <u>Variable Parameters</u><br/> <math>F_{nL}</math>, <math>L/\nabla^{1/3}</math>, <math>B/T</math>, <math>L/B</math>, <math>C_P</math><br/>                 * for one model <math>\beta_T = 20^\circ</math><br/>                 **for one model <math>i_c = 21^\circ</math></p> |

**APPENDIX B**

Table of Calm Water, Minimum Bare Hull R/W for Notional 500 mt Hull Forms

Notes:  $C_F$  – ATTC 1947 Formulation;  $C_A = 0$ ; some conditions may be dynamically unstable.

| Hull Form    | $L/\nabla^{1/3}$ | $F_{nL}$ |        |        |        |        |        |        |
|--------------|------------------|----------|--------|--------|--------|--------|--------|--------|
|              |                  | 0.4      | 0.5    | 0.6    | 0.7    | 0.8    | 0.9    | 1.0    |
| Hard Chine   | 4.0              | 0.0380   | 0.0895 | 0.1400 | 0.1475 | 0.1400 | 0.1335 | 0.1260 |
|              | 4.5              | 0.0380   | 0.0850 | 0.1185 | 0.1205 | 0.1175 | 0.1130 | 0.1055 |
|              | 5.0              | 0.0375   | 0.0785 | 0.1050 | 0.1090 | 0.1085 | 0.1075 | 0.1025 |
|              | 5.5              | 0.0375   | 0.0690 | 0.0895 | 0.0970 | 0.1005 | 0.1030 | 0.1020 |
|              | 6.0              | 0.0380   | 0.0640 | 0.0800 | 0.0875 | 0.0930 | 0.0990 | 0.1010 |
|              | 6.5              | 0.0370   | 0.0605 | 0.0745 | 0.0820 | 0.0875 | 0.0960 | 0.1005 |
|              | 7.0              | 0.0370   | 0.0585 | 0.0710 | 0.0780 | 0.0850 | 0.0945 | 0.1015 |
|              | 7.5              | 0.0375   | 0.0555 | 0.0665 | 0.0755 | 0.0850 | 0.0965 | 0.1040 |
|              | 8.0              | 0.0370   | 0.0525 | 0.0605 | 0.0720 | 0.0865 | 0.0985 | 0.1085 |
| 8.5          | 0.0350           | 0.0485   | 0.0570 | 0.0690 | 0.0850 | 0.1025 | 0.1135 |        |
| Double Chine | 6.5              | 0.0450   | 0.0625 | 0.0700 | 0.0765 | 0.0835 | 0.0935 | 0.1025 |
|              | 7.0              | 0.0400   | 0.0565 | 0.0650 | 0.0740 | 0.0815 | 0.0910 | 0.1020 |
|              | 7.5              | 0.0360   | 0.0510 | 0.0615 | 0.0695 | 0.0775 | 0.0875 | 0.1030 |
|              | 8.0              | 0.0350   | 0.0475 | 0.0585 | 0.0665 | 0.0765 | 0.0880 | 0.1055 |
|              | 8.5              | 0.0350   | 0.0475 | 0.0570 | 0.0650 | 0.0765 | 0.0915 | 0.1085 |
| Round Bilge  | 4.5              | 0.0210   | 0.0690 | 0.1080 | 0.1160 | ---    | 0.1360 | ---    |
|              | 5.0              | 0.0250   | 0.0685 | 0.0930 | 0.1000 | 0.1070 | 0.1135 | 0.1320 |
|              | 5.5              | 0.0250   | 0.0625 | 0.0810 | 0.0885 | 0.0940 | 0.1000 | 0.1090 |
|              | 6.0              | 0.0240   | 0.0565 | 0.0700 | 0.0800 | 0.0865 | 0.0935 | 0.1035 |
|              | 6.5              | 0.0230   | 0.0510 | 0.0625 | 0.0725 | 0.0810 | 0.0890 | 0.1015 |
|              | 7.0              | 0.0230   | 0.0455 | 0.0565 | 0.0665 | 0.0765 | 0.0850 | 0.1005 |
|              | 7.5              | 0.0210   | 0.0415 | 0.0523 | 0.0620 | 0.0725 | 0.0820 | 0.1020 |
|              | 8.0              | 0.0200   | 0.0375 | 0.0480 | 0.0590 | 0.0700 | 0.0795 | 0.1035 |
|              | 8.5              | 0.0195   | 0.0355 | 0.0460 | 0.0565 | 0.0683 | 0.0785 | ---    |
|              | 9.0              | 0.0185   | 0.0335 | 0.0445 | 0.0550 | 0.0665 | 0.0790 | ---    |
|              | 9.5              | 0.0180   | 0.0325 | 0.0435 | 0.0535 | 0.0650 | 0.0805 | ---    |
|              | 10.0             | 0.0175   | 0.0320 | 0.0430 | ---    | ---    | ---    | ---    |